J. Appl. Comput. Mech., 6(SI) (2020) 1364-1370
DOI: 10.22055/JACM.2020.33956.2379

ISSN: 2383-4536
jacm.scu.ac.ir

Shahid Chamran University of Ahvaz

Journal of Applied and Computational Mechanics

Research Paper

Singular Stresses at a Vertex and Along a Singular Line in Three-dimensional Piezoelectric Bonded Joints

Chonlada Luangarpa[1], Hideo Koguchi[2]

[1] Faculty of Engineering, Thammasat University (Pattaya Campus), 39/4 Tambon Pong, Amphoe Bang Lamung, Chonburi 20150, Thailand, Email: lchonlad@engr.tu.ac.th

[2] Niigata Institute of Technology, 1719 Fujihashi, Kashiwazaki City, Niigata 945-1195, Japan, Email: hkoguchi@niit.ac.jp

Received July 09 2020; Revised August 20 2020; Accepted for publication August 21 2020.
Corresponding author: C. Luangarpa (lchonlad@engr.tu.ac.th)

Abstract. Singular stress fields in three-dimensional piezoelectric bonded joints are investigated at a vertex and along a free edge (the singular line) of an interface. Two perfectly bonded joints, which are different in the side surface shapes, are considered. The joints consist of multi-terms of singularity. Two-major terms of singularity are investigated in details. The orders of singularity at the vertex and along the singular line are calculated using three-dimensional finite element eigen-analysis. The intensities of singularity are calculated using the conservative integral. The intensities of singularity at several points located on the singular line are examined. The relationships between the intensities of singularity and the distances from the vertex are plotted to determine how the vertex singularity affects the singularity along the singular line. Finally, the relationships between singular stress fields at the vertex and along the singular line are considered.

Keywords: Piezoelectric bonded joint, Singular stress, Intensity of singularity, Conservative integral.

1. Introduction

Recently, piezoelectric materials have been widely used in advance engineering and technology products, e.g., sensors or actuators. Piezoelectric bonded joints can be found in various devices. As it is known, dissimilar material bonded joints have stress singularities created by mismatched in material properties across interfaces. The stress singularities may lead to fracture and failure. Hence, it is important to investigate singular stresses of dissimilar material bonded joints.

Analysis of singularity characteristics for piezoelectric materials might be more complicated than that of non-piezoelectric materials. In addition to the mechanical behaviors, electrical properties; for example, piezoelectric constants or dielectric constants, should be considered. There are several studies on the singularity behavior of piezoelectric bonded joints [1-3]. Most of those studies are on the analysis of the order of singularity. The studies on the determination of the intensities of singularity are limited. Furthermore, for three-dimensional problems, relationship between the singularities at vertex and its side surfaces is not yet understood.

In the present study, the singular stress fields in three-dimensional piezoelectric bonded joints with multi-term of singularity are investigated in details. The order of singularity and the intensity of singularity are two major parameters to understand the singularity characteristics. The orders of singularity are calculated using the three-dimensional finite element eigen-analysis [2, 4]. The intensities of singularity are calculated using the conservative integral based on the Betti reciprocal principle. The conservative integral was first developed for calculating the stress intensity factor of notched homogeneous bodies [5-7]. The method was extended to analyse two-dimensional dissimilar material joints later [8-10]. Refer to previous studies, the conservative integral was proved to be a powerful method for calculating the intensity of singularity. In addition, a major advantage of this method is that the intensity of singularity for each term of singularity can be calculated separately. Lately, several studies extended the conservative integral to solve three-dimensional problems [11-13]. For three-dimensional dissimilar material joints, Luangarpa and Koguchi [14] were developed the conservative integral for calculating the intensity of singularity at a vertex of three-dimensional bonded joint with one real singularity. And then, the method is extended to calculating the intensities of singularity along the singular line of the bonded joints [15]. That paper explain relationship between the singular stress fields at the vertex and along the singular line in case of one-real singularity. A recent study by [16] extended the method for calculating the intensity of singularity at a vertex of three-dimensional piezoelectric bonded joint with multi-terms of singularity. As shown in [15], for three-dimensional bonded joints, the singularities are generated not only at the vertices, but also along the free edges of the interface. Hence, one of the objectives of the present study is to extend the conservative integral to calculating the intensity of singularity along the singular line in case of multi-term of singularities.

In order to understand the relationship between the singularities at vertex and its side surfaces, the two models, which are different in the side surface shapes, are used. The intensities of singularities at several positions along the singular line of the interface are examined. Finally, the relationship between the singularities at vertex and that along the stress singular line is discussed.

Published online: August 28 2020

2. Analytical Methods

A conservative integral following [14] is extended to calculate the intensity of singularity along a singular line in three-dimensional piezoelectric bonded joints, as shown in Figures 1(a) and 1(b). This principle is developed using Betti's reciprocal principle as follows:

$$\int_s (T'_i u_i - T_i u'_i) ds = 0 \tag{1}$$

For any contour S, T_i and T'_i (i =1, 3) are tractions, and u_i and u'_i are the displacements of the singular and complementary fields. Considering cases of piezoelectric material, additional terms related to electric properties are added; T_4 and T'_4 are the electric displacements with the outward unit vector ($T_4 = \sigma_{4j}\hat{n}_j$), and u_4 and u'_4 are the electric potentials of the singular and complementary fields.
Equation (1) is rewritten as an integral with respect to the closed area shown in Figure 2(a) as follows:

$$\sum_{k=0}^{n} \int_{S_k} (T'_i u_i - T_i u'_i) ds = 0 \tag{2}$$

The contour, S, is composed of S_k (k = 0, 3), where S_2 and S_3 are on free-surfaces. Then, the tractions are zero on these surfaces such that

$$\int_{S_0} (T'_i u_i - T_i u'_i) ds + \int_{S_1} (T'_i u_i - T_i u'_i) ds = 0 \tag{3}$$

Modifying the form of traction to be $T_i = \sigma_{ij}\hat{n}_j$, where $\hat{n}_j$ is the outward unit vector to the closed surface, S. Let $\hat{n}'_j$ be the unit vector in the reversed direction of $\hat{n}_j$, such that

$$\int_{S_0} (\sigma'_{ij} u_i - \sigma_{ij} u'_i)\hat{n}'_j ds = \int_{S_1} (\sigma'_{ij} u_i - \sigma_{ij} u'_i)\hat{n}_j ds \tag{4}$$

Equation (4) demonstrates that the integral is an area independent integral. Finally, the H-integral at the vertex in three-dimensional dissimilar materials is defined as follows:

$$H = \int_{S_\Gamma} (\sigma'_{ij} u_i - \sigma_{ij} u'_i)\hat{n}_j ds \tag{5}$$

where S_Γ is an arbitrary surface area enclosing the singular point (see Figure 2(b)). The asymptotic stresses around the singular point in the spherical coordinate system can be described as follows:

$$\sigma_{ij}(r,\theta,\phi) = \sum_{n=1}^{m} K_n \left(\frac{r}{L}\right)^{-\lambda_n} f_{ij}^{(n)}(\theta,\phi) \tag{6}$$

where (i, j = r, θ, ϕ), r is the radial distance from the singular point, L is a model length, K_n is the intensity of singularity, λ_n is the order of the stress singularity, f_{ij} is the angular function of stress, and m is the number of singularity term. The displacement fields are given by

$$u_i(r,\theta,\phi) = \sum_{n=1}^{m} K_n \left(\frac{r^{1-\lambda_n}}{L^{-\lambda_n}}\right) g_i^{(n)}(\theta,\phi) \tag{7}$$

where u_i is the displacement, and g_i is the angular function of displacement. Equations (6) and (7) are the same as the equations of non-piezoelectric material. For piezoelectric material, additional equations related to electric properties shall be considered. The asymptotic electric displacement and electric potential are written as follows:

$$\sigma_{4j}(r,\theta,\phi) = \sum_{n=1}^{m} K_n \left(\frac{r}{L}\right)^{-\lambda_n} f_{4j}^{(n)}(\theta,\phi) \tag{8}$$

$$u_4(r,\theta,\phi) = \sum_{n=1}^{m} K_n \left(\frac{r^{1-\lambda_n}}{L^{-\lambda_n}}\right) g_4^{(n)}(\theta,\phi) \tag{9}$$

where σ_{4j} and u_4 are the electric displacement and the electric potential, f_{4j} is the angular function of electric displacement, and g_4 is the angular function of electric potential.
In the present study, two major-terms of singularity are investigated, then m = 2 is defined. Following [16], the stresses and electric displacements are simplified to be the unified singular equation with two-term of singularities as:

$$[\boldsymbol{\sigma}(r,\theta,\phi)] = [\boldsymbol{f}(\theta,\phi)]\left[\left(\frac{r}{L}\right)^{-\lambda}\right][\boldsymbol{K}] \tag{10}$$

where

$$[\boldsymbol{\sigma}(r,\theta,\phi)] = \begin{Bmatrix} \sigma_{rr}(r,\theta,\phi) \\ \sigma_{\theta\theta}(r,\theta,\phi) \\ \sigma_{\phi\phi}(r,\theta,\phi) \\ \tau_{r\theta}(r,\theta,\phi) \\ \tau_{r\phi}(r,\theta,\phi) \\ \tau_{\theta\phi}(r,\theta,\phi) \\ D_r(r,\theta,\phi) \\ D_\theta(r,\theta,\phi) \\ D_\phi(r,\theta,\phi) \end{Bmatrix}, [\boldsymbol{f}(\theta,\phi)] = \begin{bmatrix} f_{rr}^{(1)}(\theta,\phi) & f_{rr}^{(2)}(\theta,\phi) \\ f_{\theta\theta}^{(1)}(\theta,\phi) & f_{\theta\theta}^{(2)}(\theta,\phi) \\ f_{\phi\phi}^{(1)}(\theta,\phi) & f_{\phi\phi}^{(2)}(\theta,\phi) \\ f_{r\theta}^{(1)}(\theta,\phi) & f_{r\theta}^{(2)}(\theta,\phi) \\ f_{r\phi}^{(1)}(\theta,\phi) & f_{r\phi}^{(2)}(\theta,\phi) \\ f_{\theta\phi}^{(1)}(\theta,\phi) & f_{\theta\phi}^{(2)}(\theta,\phi) \\ f_{4r}^{(1)}(\theta,\phi) & f_{4r}^{(2)}(\theta,\phi) \\ f_{4\theta}^{(1)}(\theta,\phi) & f_{4\theta}^{(2)}(\theta,\phi) \\ f_{4\phi}^{(1)}(\theta,\phi) & f_{4\phi}^{(2)}(\theta,\phi) \end{bmatrix}, \left[\left(\frac{r}{L}\right)^{-\lambda}\right] = \begin{bmatrix} \left(\frac{r}{L}\right)^{-\lambda_1} & 0 \\ 0 & \left(\frac{r}{L}\right)^{-\lambda_2} \end{bmatrix}, [\boldsymbol{K}] = \begin{Bmatrix} K_1 \\ K_2 \end{Bmatrix}$$

Table 1. Material Properties.

		PZT-4	PZT-5H
Elastic Constant, GPa	C_{11}	139	126
	C_{12}	77.8	55
	C_{13}	74.3	53
	C_{33}	113	117
	C_{44}	25.6	35.3
Piezoelectric Constant, C/m^2	e_{31}	-6.98	-6.5
	e_{33}	13.8	23.3
	e_{15}	13.4	17.0
Dielectric Constant, 10^{-10} C/Vm	χ_{11}	60.0	151
	χ_{33}	54.7	130

Determination of each intensity of singularity is obtained by calculated the stresses and displacements for each order of singularity as follows:

$$\sigma_{ij}^{(n)}(r,\theta,\phi) = K_n\left(\frac{r}{L}\right)^{-\lambda_n} f_{ij}^{(n)}(\theta,\phi) \tag{11}$$

$$u_i^{(n)}(r,\theta,\phi) = K_n\left(\frac{r^{1-\lambda_n}}{L^{-\lambda_n}}\right) g_i^{(n)}(\theta,\phi) \tag{12}$$

The primed solution is a complementary solution with an order of singularity of λ`= 3-λ. The stress components and the displacements are given by

$$\sigma'^{(n)}_{ij}(r,\theta,\phi) = C_n\left(\frac{r}{L}\right)^{-\lambda'_n} f'^{(n)}_{ij}(\theta,\phi) \tag{13}$$

$$u'^{(n)}_i(r,\theta,\phi) = C_n\left(\frac{r^{1-\lambda'_n}}{L^{-\lambda'_n}}\right) g'^{(n)}_i(\theta,\phi) \tag{14}$$

Finally, the intensity of singularity can be obtained from

$$K_n = H = \int_{S_\Gamma}(\sigma'^{(n)}_{ij}u_i - \sigma_{ij}u'^{(n)}_i)\hat{n}_j ds \tag{15}$$

where S_Γ is an arbitrary surface area enclosing the singular point.

3. Models for Analysis

Two models are used in the present study. Both models are bi-material bonded joints between PZT-4 and PZT-5H, which the poling direction is parallel to the z-axis. The vertices are considered to be the intersection between two side surfaces. The side surfaces are considered to be dissimilar material bonded lines (singular lines). For Model-1 (see Figure 1(a)), both side surfaces are; θ = 0-90° for PZT-4 and θ = 90-270° for PZT-5H. The singular line on this side surface is called Line-1 (step surface). For Model-2 (see Figure 1(b)), one line is the same as Model-1 (θ = 0-90° for PZT-4 and θ = 90-270° for PZT-5H), the other is; θ = 0-90° for PZT-4 and θ = 90-180° for PZT-5H, which is called Line-2 (flat surface). The intersections between two side surfaces for Model-1 and Model-2 are called Vertex-1 and Vertex-2, respectively. Both models are analysed under the same boundary conditions. A uniform tensile stress ($\sigma_0 = 10$ MPa), is applied to the top surface. The model is fixed on the bottom surface. The length, L, is fixed at 5 mm. Dimensions and boundary conditions are shown in Figures 1(a) and 1(b). The material properties are listed in Table 1.

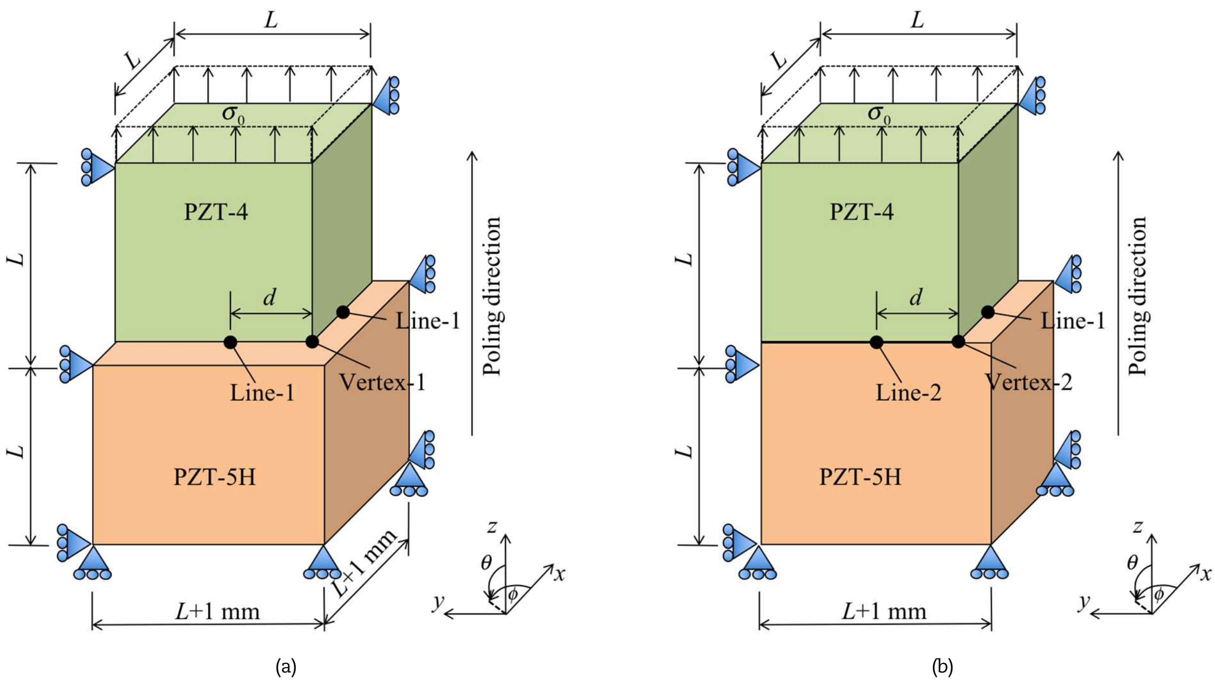

Fig. 1. Piezoelectric bonded joint models used in the present study; (a) Model-1 and (b) Model-2

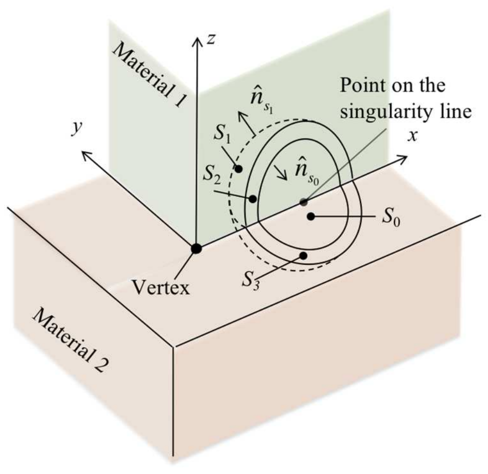

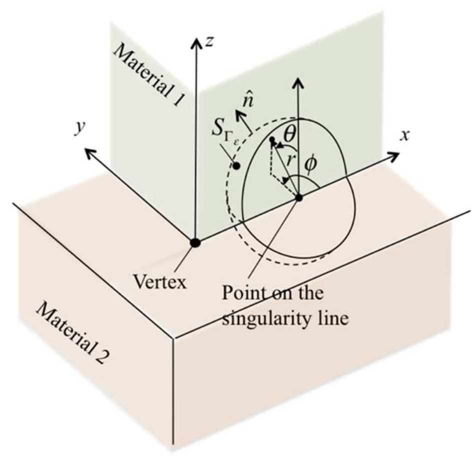

Fig. 2. (a) A specific closed area for integral, (b) A small circle area, S_Γ

4. Numerical Results

4.1 Orders of Singularity and Angular Functions

Eigen analysis formulated by a three-dimensional FEM is used to calculate the orders of stress singularity [2, 4]. The eigen equation derived by the principle of virtual work for calculating the eigenvalue, p, is expressed as follows:

$$(p^2[\mathbf{A}] + p[\mathbf{B}] + [\mathbf{C}])\{\mathbf{u}\} = 0 \tag{16}$$

where $[\mathbf{A}]$, $[\mathbf{B}]$, and $[\mathbf{C}]$ are matrices composed of material properties, $p = 1 - \lambda$, and $\{\mathbf{u}\}$ is the eigenvector of displacement and electric potential.

Table 2 presents the results for the orders of the singularity at the vertices, $\lambda_{vertex}^{(v,n)}$; where v = 1 for Vertex-1, and v = 2 for Vertex-2 and n is n-term of singularity. The results show that both models consist of multi-term of singularities at the vertex. As mention before, two-major terms of singularities are considered, and $\lambda^{(m,1)}$ is defined to be the order of singularity that is the largest value. The values of the orders of the singularity of Vertex-1 are larger than that of Vertex-2.

Next, values of the orders of the singularity along the singular line, $\lambda_{line}^{(l,n)}$; where l = 1 for Line-1, and l = 2 for Line-2, are presented in Tables 3. The results in Table 3 shows that the values of the orders of the singularity of Line-2 are very small. Then, Line-2 is considered to be the bonded joint without singularity.

These results mean that Vertex-1 is the combination of two singular side surfaces. In the other hand, Vertex-2 is the combination of one singular side surface and one non-singular side surface. For Model-1, the value of $\lambda_{vertex}^{(1,1)}$ is larger than that of $\lambda_{line}^{(1,1)}$. However, the values of $\lambda_{vertex}^{(1,2)}$ and $\lambda_{line}^{(1,2)}$ are nearly the same value. For Model-2, the values of $\lambda_{vertex}^{(2,1)}$ and $\lambda_{vertex}^{(2,2)}$ are both smaller than that of $\lambda_{line}^{(1,1)}$ and $\lambda_{line}^{(1,2)}$, respectively. It may be considered that the vertex singularity is the combination of two singularity along the singular line (two sides meet).

After calculated the orders of the singularity, the angular functions of the displacements and the electric potential, $g_i(\theta,\phi)$ and $g'_i(\theta,\phi)$, shown in Eqs. (12) and (14) are obtained using eigenvector analysis. The angular functions of the displacements and the electric potential are then converted to the angular functions of the stresses and the electric displacements, $f_{ij}(\theta,\phi)$ and $f'_{ij}(\theta,\phi)$, shown in Eqs. (11) and (13) following the stress-strain relation.

The angular functions at the vertex are normalized such that

$$f_{\theta\theta vertex}^{(n)}\left(\frac{\pi}{2},\frac{\pi}{4}\right) = 1,\ \ f'^{(n)}_{\theta\theta vertex}\left(\frac{\pi}{2},\frac{\pi}{4}\right) = 1 \tag{17}$$

Details of the eigenvalue, the eigenvector analysis and the angular functions at the vertex are shown in [16].

Next, the angular functions for the point on the singular line are normalized such that

$$f_{\theta\theta line}^{(n)}\left(\frac{\pi}{2},\frac{\pi}{2}\right) = 1, \qquad f'^{(n)}_{\theta\theta line}\left(\frac{\pi}{2},\frac{\pi}{2}\right) = 1 \tag{18}$$

Table 2. The order of stress singularities at the vertices, $\boldsymbol{\lambda_{vertex}^{(v,n)}}$.

	Vertex-1 $\left(\lambda_{vertex}^{(1,n)}\right)$	Vertex-2 $\left(\lambda_{vertex}^{(2,n)}\right)$
$\lambda_{vertex}^{(v,1)}$	0.587	0.356
$\lambda_{vertex}^{(v,2)}$	0.313	0.275
$\lambda_{vertex}^{(v,3)}$	0.178	0.214

Table 3. The order of stress singularities along the singular line, $\boldsymbol{\lambda_{line}^{(l,n)}}$.

	Line-1 $\left(\lambda_{line}^{(1,n)}\right)$	Line-2 $\left(\lambda_{line}^{(2,n)}\right)$
$\lambda_{line}^{(l,1)}$	0.478	0.033
$\lambda_{line}^{(l,2)}$	0.366	0.000
$\lambda_{line}^{(l,3)}$	0.333	0.000

Table 4. The intensities of singularities at the vertices, $K_{vertex}^{(m,n)}$.

	Vertex-1 $\left(K_{vertex}^{(1,n)}\right)$	Vertex-2 $\left(K_{vertex}^{(2,n)}\right)$
$K_{vertex}^{(m,1)}$	1.06	1.31
$K_{vertex}^{(m,2)}$	1.87	2.25

4.2 Intensities of singularity

The conservative integral is used to calculate the intensity of singularity at the vertices (Vertex-1 and Vertex-2. The intensities of singularities at the vertices are presented in Table 4. (Details of the conservative integral for the vertex are presented in [16].) The results indicated that the values of intensities of singularities of Model-2 are larger than that of Model-1. However, the magnitudes of stresses approached to Vertex-2 may not be as large as Vertex-1 since the values of the orders of singularities of Vertex-2 are smaller than that of Vertex-1.

Next, the conservative integral is extended to obtain the intensity of the singularity at several points located on the singular lines (Line-1 in Model-1 and Model-2). Example of the mesh models (the models with d = 2 mm, where d is the distance from the vertex) used in the FE analysis is shown in Figure 3(a) and 3(b) for Model-1 and Model-2, respectively. The eight-node element is used in the same manner as in the analysis at the vertex. The elements around the singular point are organized to be spherical shape. Similar to the analysis at the vertex, the angular dimensions of the element are ϕ = 15° and θ = 15°; and the size of the smallest element connected to the singular point is 0.01 mm in the r-direction. The integral surface area is the area with a distance 0.05 mm from the investigated point.

Figs. 4(a) and 4(b) shows the values of $K_{line}^{(1)}$ and $K_{line}^{(2)}$ with (d/L), for Model-1 and Model-2, respectively. The results from both models indicated that $K_{line}^{(1)}$ and $K_{line}^{(2)}$ approach constant values at the points further from the vertex. In addition, the values of $K_{line}^{(1)}$ are much larger than that of $K_{line}^{(2)}$. That means we may predict the singular fields along the singular line by considering only the first-term of singularity. For Model-1, $K_{line}^{(1)}$ increases greatly as Vertex-1 approaches. In contrast, for Model-2, $K_{line}^{(1)}$ decreases as Vertex-2 approaches.

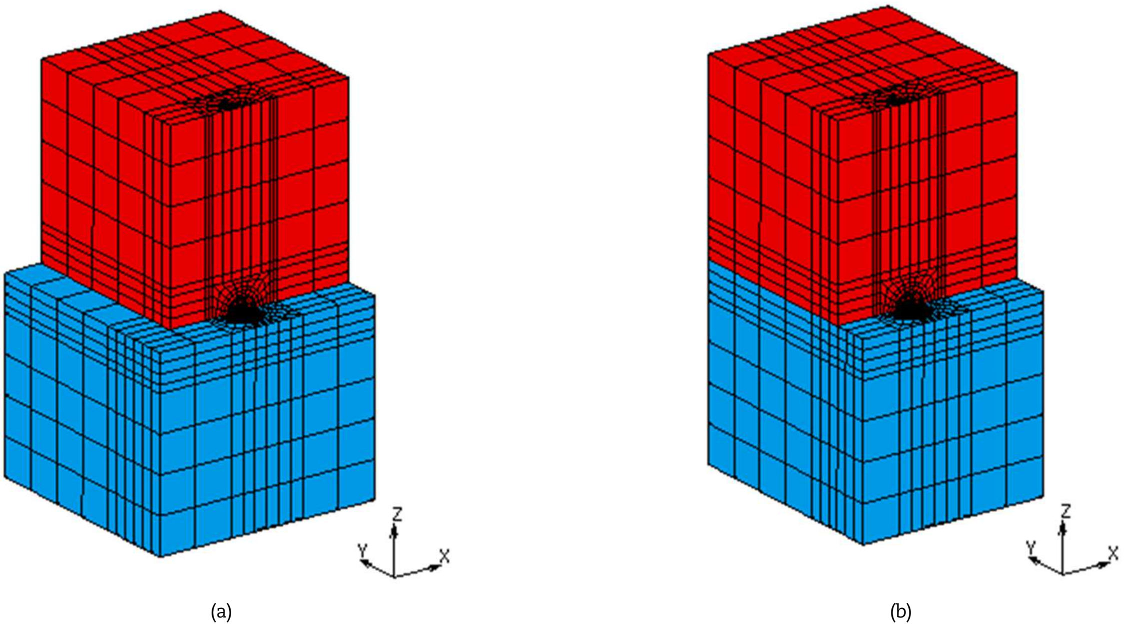

Fig. 3. Mesh models for FE analysis at the point (d = 2 mm) on the singular line; (a) Model-1, (b) Model-2.

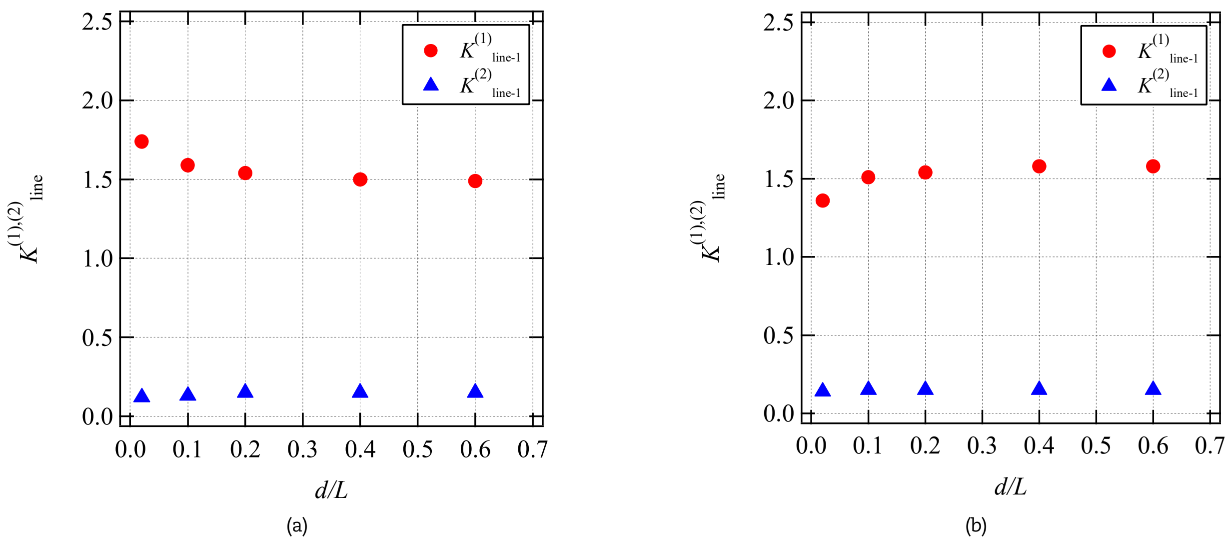

Fig. 4. The intensity of singularity on the singular lines with d/L for (a) Model-1 and (b) Model-2.

5. Discussion

From the results of the orders of singularities, it was observed that the value of the 1st-order of singularity at the vertex of Model-1 ($\lambda^{(1,1)}_{vertex}$), which two singular side surfaces meet, is larger than the value of the 1st-order of singularity along the singular line ($\lambda^{(1,1)}_{line}$). On the other hand, the values of the order of singularity at the vertex of Model-2 (both $\lambda^{(2,1)}_{vertex}$ and $\lambda^{(2,2)}_{vertex}$), which is the combination between singular side surface and non-singular side surface, are smaller than its values along the singular line, and also smaller than that of Model-1.

In addition, the difference between the values of the intensities of singularities at several points along the singularity lines of Model-1 and Model-2 indicated that, as the vertex approached, the singularity increases for Model-1 and decreases for Model-2. These results are consistent with the results of the orders of singularities. This means that the vertex singularity may be considered to be summation of the side surface singularity.

In order to confirm the present finding, the stresses and the electric displacements enclosed to the vertices are plotted and compared. Figures 5(a) and 5(b) shows the distributions of stresses, $\sigma_{\theta\theta}$, at the interface, $\theta = 90°$, plot for Vertex-1 and Vertex-2 with fixed r at 0.005, 0.01 and 0.05 mm. These results indicated that the magnitude of stresses of Model-1 are larger than that of Model-2. Furthermore, the magnitudes of stress increase as approach to Line-1 and remain constant as approach to Line-2. Figures 6(a) and 6(b) shows the distributions of electric displacements, D_θ, at the interface, $\theta = 90°$, plot for Vertex-1 and Vertex-2 with fixed r at 0.005, 0.01 and 0.05 mm. These results are consistent with the distributions of stresses, and indicated that the singularity do not only associate with mechanical stresses, but also associate with the electrical behaviors.

In order to confirm the accuracy of the calculation, the stresses and the electric displacements analyzed using the conventional FEM with mesh refinement are also plotted in Figures 5(a), 5(b), 6(a) and 6(b). These figures show that the results calculated using the conservative integral have good agreement with the results calculated using the conventional FEM.

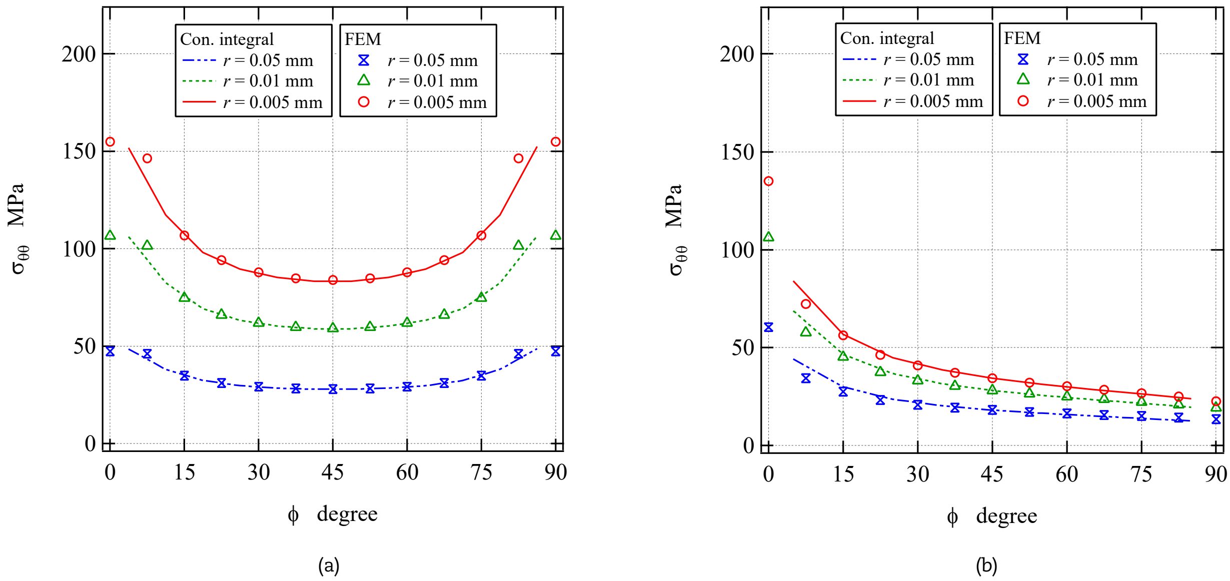

Fig. 5. Engineering stresses, $\sigma_{\theta\theta}$, at the interface, $\theta = 90°$, plot for (a) Vertex-1 and (b) Vertex-2 with fixed r at 0.005, 0.01 and 0.05 mm.

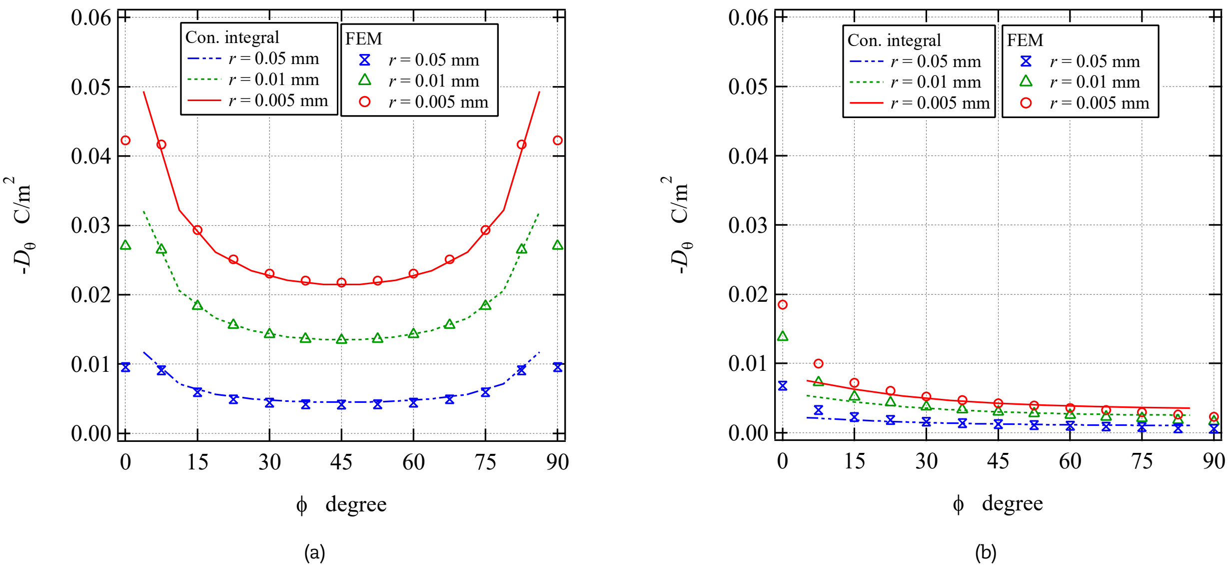

Fig. 6. Electric displacements, D_θ, at the interface, $\theta = 90°$, plot for (a) Vertex-1 and (b) Vertex-2 with fixed r at 0.005, 0.01 and 0.05 mm.

6. Conclusions

In this study, three-dimensional piezoelectric bonded joints are investigated at the vertices and along the free edges of interface. Two models, which are different in the side surface shapes, are examined to study relationship between the vertex singularity and line singularity. The results of the present study are summarized as follows:

1) The conservative integral based on the Betti reciprocal principle was extended to calculate the intensity of singularity along the singular line in three-dimensional piezoelectric-material bonded joints with multi-terms of singularities. The distributions of stresses and electric displacements compared between using the conservative integral and using the conventional FEM with mesh refinement were in good agreement.

2) The results of the orders of singularities and the intensities of the singularities for two models revealed that the stress singularity characteristics at the vertex in three-dimensional bonded joints might be described as a function of the singularity along the side surface of interface (the singular line).

3) The distributions of stresses and electric displacements enclosed to the vertices indicated that the singularity characteristics affect the electrical behaviors for the piezoelectric materials.

Author Contributions

Chonlada Luangarpa performed the numerical investigations and wrote the manuscript in consultation with Hideo Koguchi. All authors discussed the results, reviewed and approved the final version of the manuscript.

Conflict of Interest

The authors declared no potential conflicts of interest with respect to the research, authorship and publication of this article.

Funding

The authors received no financial support for the research, authorship and publication of this article.

References

[1] Chen C.D., On the singularities of the thermo-electro-elastic fields near the apex of a piezoelectric bonded wedge, *International Journal of Solids and Structures*, 43, 2006, 957-981.

[2] Islam M.S. and Koguchi H., Characteristics of Singular Stress Distribution at a Vertex in Transversely Isotropic Piezoelectric Dissimilar Material Joints, *Journal of Solid Mechanics and Materials Engineering*, 4(7), 2010, 1011-1026.

[3] Islam M.S. and Koguchi H., Analysis of Singularity at a Vertex in 3D Transversely Isotropic Piezoelectric Single-step Bonded Joints with Various Thicknesses by Boundary Element Method, *Journal of Solid Mechanics and Materials Engineering*, 6, 2012, 844-859.

[4] Pageau S.S. and Biggers Jr S. B., Finite Element Evaluation of Free-Edge Singular Stress Fields in Anisotropic Materials, *International Journal for Numerical Methods in Engineering*, 38, 1995, 2225-2239.

[5] Stern M., Becker E., and Dunham R., A contour integral computation of mixed-mode stress intensity factors, *International Journal of Fracture*, 7, 1976, 125–132.

[6] Sinclair G.B., Okajima M., and Griffin J.H., Path independent integrals for computing stress intensity factors at sharp notches in elastic plates, *International Journal for Numerical Methods in Engineering*, 20, 1984, 999-1008.

[7] Carpenter W.C., Calculation of fracture mechanics parameters for a general corner, *International Journal of Fracture*, 24, 1984, 45–58.

[8] Carpenter, W.C. and Byers C., A path independent integral for computing stress intensities for V-notched cracks in a bi-material, *International Journal of Fracture*, 35, 1987, 245–268.

[9] Banks-Sills L., A conservative integral for determining stress intensity factors of a biomaterial strip, *International Journal of Fracture*, 86, 1997, 385-398.

[10] Banks-Sills L. and Sherer A., A conservative integral for determining stress intensity factors of a biomaterial notch, *International Journal of Fracture*, 115, 2002, 1-26.

[11] Meda G., Messner T.W., Sinclair G.B. and Solecki J.S., Path-independent H integrals for three-dimensional fracture mechanics, *International Journal of Fracture*, 94, 1998, 217-234.

[12] Ortiz J.E., Mantic V. and Paris F., A domain-independent integral for computation of stress intensity factors along three-dimensional crack fronts and edges by BEM, *International Journal of Solids and Structures*, 43, 2006, 5593-5612.

[13] Nomura, Y., Ikeda, T. and Miyazaki, N., Stress intensity factor analysis of a three-dimensional interfacial corner between anisotropic bimaterials under thermal stress, *International Journal of Solids and Structures*, 47, 2010, 1775-1784.

[14] Luangarpa C., and Koguchi H., Analysis of a three-dimensional dissimilar material joint with one real singularity using a conservative integral, *International Journal of Solids and Structures*, 51, 2014, 2908-2919.

[15] Luangarpa C., and Koguchi H., Analysis of singular stresses at a vertex and along a singular line in three-dimensional bonded joints using a conservative integral, *European Journal of Mechanics - A/Solids*, 60, 2016, 208-216.

[16] Luangarpa C., and Koguchi H., Evaluation of intensities of singularity at three-dimensional piezoelectric bonded joints using a conservative integral, *European Journal of Mechanics - A/Solids*, 72, 2018, 198-208.

ORCID iD

Chonlada Luangarpa https://orcid.org/0000-0001-6051-970X

How to cite this article: Luangarpa C., Koguchi H. Singular Stresses at a Vertex and Along a Singular Line in Three-dimensional Piezoelectric Bonded Joints, *J. Appl. Comput. Mech.*, 6(SI), 2020, 1364–1370. https://doi.org/10.22055/JACM.2020.33956.2379